

## Structure of Water in Microemulsions: Electrical, Birefringence, and Nuclear Magnetic Resonance Studies

**Abstract.** *Microemulsions, which are optically transparent oil-water dispersions, were produced by mixing hexadecane, hexanol, potassium oleate, and water. As the amount of water is increased, the microemulsion exhibits a clear to turbid to clear transition. In contrast to the clear regions, the turbid region possesses birefringence. The development of birefringence is also accompanied by a sharp decrease in the electrical resistance. The high-resolution (220 megacycle) nuclear magnetic resonance data suggest that water exists in two distinct molecular environments in the birefringent region; the first environment is characterized by relatively less mobile water molecules than oil molecules, whereas in the second environment oil molecules are less mobile than water molecules. The electrical, birefringence, and nuclear magnetic resonance data are in agreement with the proposed mechanism of change in the structure of water from water spheres to water cylinders to water lamellae. The chemical shift of water protons suggests that the molecular environment of water in spheres is different from that of water in cylinders or that of water in lamellae.*

Microemulsions are optically clear, stable dispersions of oil and water usually obtained by using a variety of surface-active molecules or mixtures of molecules as emulsifiers (1, 2). Such oil-in-water or water-in-oil microemulsions have been examined by low-angle x-ray measurements (3), light scattering techniques (4), ultracentrifugation (5), electron microscopy (2), and viscosity measurements (6), and have been shown to consist of droplets 100 to 600 Å in di-

ameter. The water-in-oil type of microemulsion provides a very useful system for the study of the structure of water near charged surfaces produced by polar groups of emulsifiers. We report here the effect of an increase in the water content of microemulsions on their electrical, optical, and nuclear magnetic resonance (NMR) characteristics.

Microemulsions were produced by mixing hexadecane (oil), hexanol, and potassium oleate in a test tube in the

following proportions: for 1 ml of hexadecane, 0.4 ml of hexanol and 0.2 g of potassium oleate were added. Water was added in small amounts to this mixture, which was then shaken vigorously. Optical clarity, birefringence, electrical resistance, and NMR measurements were made upon the gradual addition of water to this mixture. Two polarizing plastic sheets were arranged perpendicular to one another to detect birefringence of the microemulsions. Two glass-sealed copper wires (0.16 cm thick) were used as electrodes. A 1-cm length at the end of each wire was exposed outside the glass tube, and the copper wires were separated by 0.8 cm. The electrical resistance of the mixture was measured by dipping the electrodes, connected to a conductivity bridge (Beckman model RC 16B2), into the microemulsions. Nuclear magnetic resonance spectra were obtained after the gradual addition of water to the microemulsion in the sample tube of the NMR spectrometer (Varian HA-220 megacycle). Tetramethylsilane was used as an internal standard. All chemicals were of high purity (> 99 percent), and the water was double-distilled.

Figure 1 shows the optical and birefringence characteristics as well as the

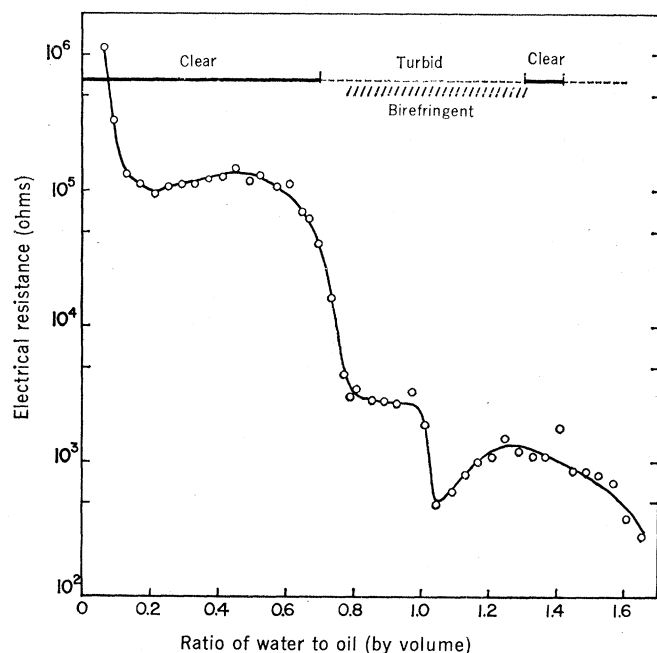
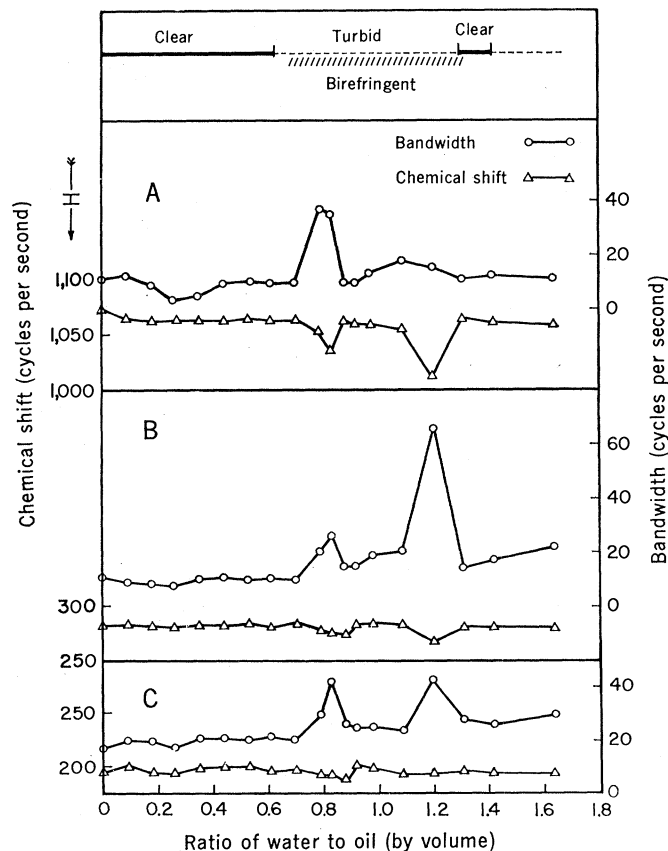


Fig. 1 (above). Variation in electrical resistance, optical clarity, and birefringence of microemulsions as the water content increases. The microemulsion contains 0.20 g of potassium oleate per milliliter of oil; the ratio of hexanol to oil is 0.40 (by volume). Fig. 2 (right). Variation in the bandwidth at half height and chemical shift of (A) water, (B) methylene, and (C) methyl protons in high-resolution NMR (220-megacycle) spectra of the same microemulsion as that in Fig. 1, as the water content increases. The upper part of the diagram shows corresponding data on optical clarity and birefringence.



measured electrical resistances as a function of the water content of the microemulsions. Figure 2 shows the chemical shifts and bandwidths at half height of the major peaks in the NMR spectra of the microemulsions. As the amount of water increases, the microemulsion passes through a clear to turbid to clear transition. In contrast to the two clear regions, the turbid region exhibits birefringence. After clarity returns for the second time, the dispersion becomes opaque, milky, and nonbirefringent (Fig. 1). The variation of the electrical resistance as a function of water content follows a very unusual pattern. For ratios of water to oil from 0.2 to 0.6, there is no significant change in the resistance. However, in the birefringent region the electrical resistance falls sharply at ratios close to 0.7 and 1.0, and subsequently it increases and then decreases (Fig. 1). The NMR data also indicate that in the birefringent region distinct changes occur in the chemical shifts and in the broadening of resonance peaks of water and hydrocarbon protons. It is evident that the chemical shift of water protons is markedly influenced in contrast to that of methylene or methyl protons (Fig. 2).

The variation in electrical resistance is explained as follows. The resistance drops from  $10^6$  to  $10^5$  ohms as the ratio of water to oil approaches 0.1; this effect is presumably due to the molecular solubilization of water in the hexadecane-hexanol-potassium oleate mixture. This interpretation is supported by the observation that the hydroxylic protons of hexanol show an upfield shift from 1175 to 1165 cycles per second with the initial addition of water. The occurrence of a single peak for hydroxylic and water protons suggests that there is a rapid rate of exchange between these protons. The constancy of resistance between the ratios 0.1 to 0.65 suggests that further addition of water results in the formation of microemulsions consisting of water spheres in the continuous oil medium, in which the interface between the oil and water is the main barrier controlling the ion-transport between the electrodes. It is expected that microemulsions having such water spheres would be nonbirefringent.

An abrupt drop in resistance in the birefringent region cannot be explained in terms of an abrupt increase in the dissociation of potassium oleate since this does not explain the development of birefringence. We propose that the sharp drop in resistance and

the development of birefringence are due to a transition in the structure of water from water spheres to water cylinders to water lamellae in this system. The NMR data, which indicate that water exists in two distinct molecular environments in the birefringent region, support this mechanism. In the first environment in the birefringent region the chemical shift of water protons moves upfield by 25 cycles per second and in the second environment by 50 cycles per second as compared to that of water spheres (Fig. 2). However, the bandwidth at half height of water protons is considerably greater in the first as compared with the second environment. The bandwidth is related to the molecular mobility or motion. In general, the greater the bandwidth, the smaller the molecular mobility. The measurements of the bandwidth at half height suggest that water molecules are less mobile or have less mobility in the first environment than in the second. In contrast to water protons, the bandwidth of methylene protons suggests that hydrocarbon chains are less mobile in the second environment than in the first. These are expected characteristics if the first environment consists of water cylinders dispersed in a continuous oil medium and the second environment consists of water and oil lamellae. Water molecules would be less mobile in the cylinders than in the lamellae. Moreover, the formation of these structures would also decrease electrical resistance since the ions could migrate within water cylinders or lamellae without passing through the oil-water interface. The formation of these structures can also account for the development of birefringence. The ratios of water to oil characterizing two distinct molecular environments on the basis of NMR data are slightly higher than those showing an abrupt decrease in electrical resistance. This effect is presumably due to the high spinning rate (6500 revolutions per minute) of the NMR sample tube, which may provide enough mechanical energy to shift the transition of water spheres to water cylinders to a higher ratio of water to oil.

The most interesting finding is the observation that the chemical shift of water when water is distributed as spheres is different from that of water distributed as cylinders or lamellae. It can be suggested from the upfield chemical shifts of water protons (Fig. 2) that the energy required to flip the proton spin is in the following order: wa-

ter spheres < water cylinders < water lamellae. This ordering is of considerable interest in relation to water in membranes and other biological systems.

The existence of such water cylinders of diameter 10 to 35 Å and lamellae 5 to 30 Å thick has been established in various lipid-water systems (7). Zlochower and Schulman (8) have shown that tight packing of hydrocarbon chains in the lamellar structure causes extreme broadening of the methylene peak in the NMR spectra. The molecular environments of these water cylinders and lamellae are not similar to that of polywater since, in contrast to the water cylinders and lamellae, the polywater exhibits a downfield shift as compared with that of normal water in the NMR spectra (9).

From electrical and birefringence data we suggest that the two clear isotropic regions represent, respectively, a water-in-oil and an oil-in-water type of microemulsion. It is expected that, as the amount of water increases, the lamellar structure will break down and the water will form a continuous phase containing microdroplets of oil stabilized by potassium oleate and hexanol. The increase in electrical resistance above a ratio of water to oil of 1.0 is mainly due to the disruption of the lamellar structures, and the subsequent decrease above a ratio of 1.3 can be attributed to the formation of a continuous water phase (clear isotropic region). Therefore, the transition from water spheres to water cylinders to water lamellae to a continuous water phase represents the mechanism of phase inversion in microemulsions. However, it should be emphasized that the formation of such structures depends upon the concentration of emulsifiers, which, in turn, determines the area available per surface-active molecule at the oil-water interface (10). Recently Ohki and Aono (11) have reported theoretical considerations for the formation of such structures in lipid-water systems. Phase inversion may result in a macro or a micro system, and the birefringent region may be transparent or turbid, with the degree of turbidity dependent upon the chemical constitution of the system. The transition from lipid spheres to lipid cylinders to lipid lamellae is known for soaps (12). In this report we describe such transition for water. We have considered other possible phases of lipid-water systems, but the proposed structures are the only ones that are supported by electrical, birefringence,

and NMR data. It should be mentioned that the viscosity of the microemulsions abruptly changes when water cylinders and lamellae are formed, and that the birefringent region is viscoelastic (13).

The chemical shift of water when it forms the continuous phase is the same as that of water when it is dispersed in spherical form. This result implies that the molecular environment of water in spherical droplets in microemulsions is the same as that of normal water and that the polar groups of surface-active molecules do not significantly alter the molecular environment. However, Cratin and Robertson (14) have reported that the chemical shift of solubilized water is different from that of emulsified water.

DINESH O. SHAH  
ROY M. HAMLIN, JR.

Departments of Chemical Engineering  
and Anesthesiology, University of  
Florida, Gainesville 32601

#### References and Notes

1. J. H. Schulman, W. Stoeckenius, L. Prince, *J. Phys. Chem.* **63**, 1677 (1959).
2. W. Stoeckenius, J. H. Schulman, L. Prince, *Kolloid Z.* **169**, 170 (1960).

3. J. H. Schulman and D. P. Riley, *J. Colloid Sci.* **3**, 383 (1948).
4. J. H. Schulman and J. A. Friend, *ibid.* **4**, 497 (1949).
5. J. E. L. Bowcott and J. H. Schulman, *Z. Elektrochem.* **59**, 283 (1955).
6. C. E. Cooke and J. H. Schulman, in *Surface Chemistry* (Proceedings of the Second Scandinavian Symposium on Surface Activity, 1964) (Munksgaard, Copenhagen, 1965); J. E. L. Bowcott, thesis, Cambridge University, Cambridge, England (1957).
7. V. Luzzati and F. Husson, *J. Cell Biol.* **12**, 207 (1962); L. Mandell, K. Fontell, P. Ekwall, *Advan. Chem. Ser.* **63**, 89 (1967); P. Ekwall, L. Mandell, K. Fontell, *Acta Chem. Scand.* **22**, 373 (1968).
8. I. A. Zlochower and J. H. Schulman, *J. Colloid Interface Sci.* **24**, 115 (1967).
9. T. F. Page, Jr., R. J. Jakobsen, E. R. Lippincott, *Science* **167**, 51 (1970); G. A. Petsko, *ibid.*, p. 171.
10. D. O. Shah, in preparation.
11. S. Ohki and O. Aono, *J. Colloid Interface Sci.* **32**, 270 (1970).
12. J. W. McBain and W. W. Lee, *Oil Soap Chicago* **20**, 17 (1943); K. D. Lawson and T. J. Flautt, *Mol. Crystallogr.* **1**, 241 (1966).
13. J. W. Falco and D. O. Shah, in preparation.
14. P. D. Cratin and B. K. Robertson, *J. Phys. Chem.* **69**, 1087 (1965).
15. We thank Professors R. D. Walker and J. H. Modell, Drs. O. A. Roels and G. Sharma, E. J. Murphy, and Mrs. P. Kilian for various comments and assistance. Part of the work was carried out at Columbia University and was supported by the Federal Water Quality Administration (grant No. WP 15080 EMP). We are grateful to the University Consortium for the use of 220-megacycle NMR spectrometer.

24 August 1970; revised 23 October 1970 ■

## Xenon Hexafluoride: Structural Crystallography of Tetrameric Phases

**Abstract.** Three crystalline phases of xenon hexafluoride are based on tetrameric association of  $\text{XeF}_6^+$  and  $\text{F}^-$  ions into eight-membered rings. Phase I (monoclinic, 8  $\text{XeF}_6$  units per cell) transforms at  $\sim 10^\circ\text{C}$  to phase II (orthorhombic, 16  $\text{XeF}_6$  units per cell), which in turn transforms at  $\sim -25^\circ\text{C}$  to phase III (monoclinic, 64  $\text{XeF}_6$  units per doubly primitive cell). The transformation from phase I to phase II requires gross reorientation of half of the tetramers in the structure. The transformation from phase II to phase III involves only an ordering of right-handed and left-handed configurations.

Recent developments are clarifying the complexities associated with  $\text{XeF}_6$  in the solid state. Heat capacity measurements (1) indicated the existence of three phases, designated I, II, and III in order of decreasing temperature, with transitions at  $19^\circ$  and  $-19^\circ\text{C}$ . A structure analysis (2) of the cubic phase (3) showed that it was an additional phase, designated IV, which is stable from the melting point to at least  $-180^\circ\text{C}$  (4). Phase I is monoclinic (3), and phases II and III are now known to be orthorhombic and monoclinic, respectively (5). We here report structural relationships between phases I, II, and III inferred from x-ray crystallography.

Experimental details of the preparation of  $\text{XeF}_6$  and the growth of single

crystals of phase II have been presented elsewhere (2, 4, 5). The most probable space group for phase II is  $Pnma$  or  $Pn2_1a$ . To a moderate approximation the phase II cell constants bear a simple relation to the phase I cell constants:  $a_{\text{II}} \cong 2a_{\text{I}}$ ,  $b_{\text{II}} \cong b_{\text{I}}$ ,  $c_{\text{II}} \cong c_{\text{I}}$ . At  $-20^\circ\text{C}$  the cell constants are  $a_{\text{II}} = 17.01 \pm 0.04 \text{ \AA}$ ,  $b_{\text{II}} = 12.04 \pm 0.03 \text{ \AA}$ ,  $c_{\text{II}} = 8.57 \pm 0.02 \text{ \AA}$ . The calculated density is  $3.71 \text{ g cm}^{-3}$  on the assumption of 16  $\text{XeF}_6$  units per unit cell. At  $-20^\circ\text{C}$  with our x-ray cryostat  $\text{XeF}_6$  has sufficient vapor pressure so that material transport between vapor and solid occurs continuously under the conditions of an x-ray experiment. Only a limited time is available for satisfactory x-ray measurements, and these consisted of Polaroid precession photo-

graphs of the  $h0l$ ,  $h1l$ ,  $h2l$ , and  $0kl$  reflections out to  $2\theta = 50^\circ$ . We measured relative intensities of 216 reflections with the photometer, using the transmission mode on Polaroid prints. An additional 110 reflections were not measurable above background. The data contain serious limitations with respect to linearity. Corrections were made for Lorentz polarization effects.

The xenon atoms were placed in space group  $Pnma$  by trial and error; this placement was followed by least-squares refinement with isotropic thermal parameters to yield an  $R$  factor (6) of 0.23 and a weighted  $R'$  factor of 0.26. A configuration of xenon atoms results which is compatible, within experimental error, with the  $\bar{4}$  symmetry found for the tetrameric association of  $\text{XeF}_5^+$  and  $\text{F}^-$  ions in phase IV (2) and for the xenon atoms in phase I (3). Least-squares refinement in space group  $Pn2_1a$  leads to unrealistic Xe-Xe distances, and  $Pnma$  is accepted as the most probable space group. This means that the tetramer is centered on a mirror plane as in phase IV and that the structure contains right-handed and left-handed configurations (7) distributed at random. The scattering model contains four tetramers of each configuration of weight  $\frac{1}{2}$  which are superimposed.

No useful information concerning fluorine positions was obtained from difference syntheses. This is not unexpected in view of the limited quantity and quality of the available data. Fluorine positions were postulated from the tetrameric component of the phase IV structure (2). Least-squares refinement with a single thermal parameter for the fluorine atoms reduced  $R$  to 0.15 and  $R'$  to 0.18. This improvement suggests that the scattering model is largely correct in broad outline. However, the data are ill-conditioned for least-squares refinement, and no significant information about Xe-F distances was obtained. There are two  $\text{F}^-$  bridged Xe-Xe distances at  $4.10(2) \text{ \AA}$  and two at  $4.07(2) \text{ \AA}$  (estimated standard deviations are given in parentheses). There is one non-bridged Xe-Xe distance at  $4.50(2) \text{ \AA}$  and one at  $4.52(2) \text{ \AA}$ .

Figure 1A illustrates the Xe positions reported for phase I (3), and Fig. 1B shows the Xe positions of phase II. Half of the tetramers are in approximately the same orientation in either phase, whereas the other half are in grossly different orientations. Evidently a single crystal cannot maintain its integrity through either the transformation